Appl. Phys. B 27, 105–113 (1982)

Applied Physics B Photophysics and Laser Chemistry

Theory of Passively Mode-Locked cw Dye Lasers

J. Herrmann and F. Weidner

Department of Physics, University, DDR-6900 Jena, German Democratic Republic

Received 13 July 1981/Accepted 15 September 1981

Abstract. The circulation of an ultrashort light pulse in a continuously pumped mode-locked dye laser with a linear cavity configuration containing the active dye, the saturable absorber and a bandwidth-limiting element is treated. The steady-state condition that the pulse shape reproduces after each cavity round-trip leads to a nonlinear integro-differential equation for this pulse shape. An approximate method for the solution of this equation not limited to the case of low laser gain and small pulse energies is given. The stable single pulse region and characteristic pulse parameters, as energy, duration, intensity and asymmetry, are considered in dependence on the laser parameters.

PACS: 42.55, 42.60

Passively mode-locked dye lasers represent a convenient tool to generate picosecond and subpicosecond light pulses [1–6]. As a result of experimental and theoretical investigations it became apparent that the generation of ultrashort pulses occurs very rapidly in mode-locked dye lasers, and the final pulse duration is much shorter than the recovery times of the saturable absorbers employed [7–9]. The mechanism of mode-locking in dye lasers therefore is quite different from that occuring in solid-state lasers.

Theoretical studies of the mode-locked dye laser have been done in [8–16]. Employing a rate equation analysis New [8, 9] first showed that by the combined action of the saturable absorber and the active medium a rapid pulse shortening can be produced if the laser parameters are such chosen that the pulse experiences a net loss on both its leading and trailing edges (static pulse compression region). Frequency dependent phenomena are explicitly left out in this analysis, therefore, a steady-state regime cannot be reached and no statement about the final pulse duration, pulse shape etc. could be given. For the description of a steady-state pulse shape the influence of bandwidth limitation of the laser transition or of a filter element (given usually by an intracavity Fabry-Perot etalon for frequency tuning) has to be taken into consideration. A steady-state solution was found numerically by Garside and Lim [10] applying density matrix formalism. They studied mode-locking conditions by perturbation analysis and found criteria for self starting of the mode-locking process characterized by the growth of a periodic perturbation on the time-independent solution. A similar analysis applying rate equation was carried out in [11]. A simple closed analytical steady-state solution taking into account bandwidth limitation by a dispersive element was given by Haus in [13]. In this paper approximations of small pulse energy (compared with the saturation energy of the absorber and the laser medium), small gain and small loss per pass were used limiting strongly the pulse and laser parameters to a very small region.

In the present paper we study the mode-locked dye laser for more realistic and more general conditions. No limitations for the pulse energy, gain and loss are demanded and a possible asymmetry of the pulse shape is taken into account. The influence of dispersive effects within the cavity is described by a frequency filter with Lorentzian line shape.

A steady-state solution for the final pulse profile is found by the requirement that the pulse shape reproduces after one cavity round-trip. This steady-state pulse shape is described by a nonlinear integro-differential equation. Using an approximate ansatz for the pulse shape a system of transcendental equations for characteristic pulse parameters can be derived. Solving these equations numerically we obtain the pulse energy, intensity, duration and asymmetry

0721-7269/82/0027/0105/$01.80

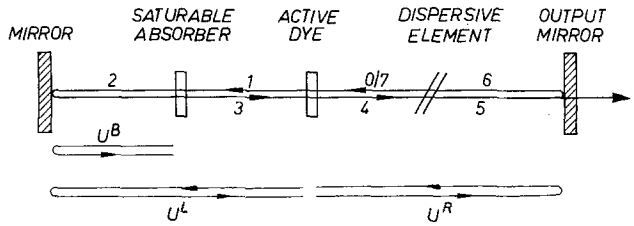

Fig. 1. Cavity configuration of the mode-locked dye laser. $U^{L,R,B}$ mark transit times of the pulse. The numbers 0–7 designate positions within the cavity

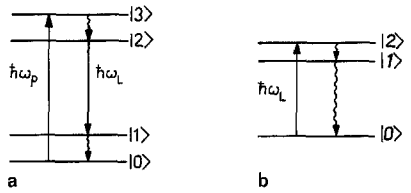

Fig. 2a and b. Level scheme of the active dye (a) and the saturable absorber (b). ω_L and ω_P are the laser and the pump frequency, respectively

in dependence on the laser parameters. Real solutions corresponding to a stable single-pulse regime are found only in a limited range of laser parameters. However this stable single-pulse region is broader than the static pulse compression region defined in [8, 14]. This means that the condition of negative net gain on both pulse edges is not a necessary condition for the pulse formation.

The numerical results show that at a certain value of the laser gain the pulse duration has a minimum. At higher pumping power the pulse duration increases again. Decreasing small signal transmission of the absorber leads to shorter and more intensive pulses with a higher pulse energy. In general, the pulse shape is asymmetric. The strength of the pulse asymmetry depends on the pump power.

1. Basic Equations

The following calculations are based on the linear cavity configuration shown in Fig. 1. We theoretically treat the steady-state regime of the laser when only a single pulse circulates within the cavity and the laser emits a continuous train of ultrashort pulses. The interaction of the laser pulse with the dye molecules is treated in the well-known semi-classical way using balance equations. The active dye is assumed to be a four-level system (Fig. 2a) with a very fast relaxation from the pump level $|3\rangle$ to the upper laser level $|2\rangle$ and from the lower laser level $|1\rangle$ to the ground state $|0\rangle$ leading to a negligible population of the levels $|3\rangle$ and $|1\rangle$. The absorber is regarded as a three-level system (Fig. 2b) with negligible population of the excited vibrational level $|2\rangle$ of the S_1 electronic state. The laser frequency ω_L determined by the dispersive element in the cavity is assumed to lie not too far away from the center frequency of the absorber and laser transition. This condition allows to neglect spatial and temporal changes in the phase of the laser pulse during the passage through the media in the cavity.

The changes of the photon flux density F and the population difference in the active medium $\Delta n^a = n_2^a$ and the absorber $\Delta n^b = n_0^b - n_1^b$ are described by the rate equations

$$\frac{\partial F}{\partial \xi} = \sigma^a \Delta n^a F, \tag{1a}$$

$$\frac{\partial}{\partial \eta}\Delta n^a = -\sigma^a \Delta n^a F + \frac{\Delta n_0^a - \Delta n^a}{T_1^a}, \tag{1b}$$

$$\frac{\partial F}{\partial \xi} = -\sigma^b \Delta n^b F, \tag{2a}$$

$$\frac{\partial}{\partial \eta}\Delta n^b = -\sigma^b \Delta n^b F + \frac{\Delta n_0^b - \Delta n^b}{T_1^b}. \tag{2b}$$

Here the quantities refering to the active medium are denoted by the index a, those referring to the saturable absorber by the index b. The variables are $\xi = z$ and $\eta = t - (z/V_{gr})$, where z is the space coordinate in the propagation direction of the pulse and V_{gr} is the group velocity in the medium. σ is the absorption cross section and

T_1 the recovery time to the equilibrium population difference Δn_0. T_1^a and T_1^b are long compared with the pulse duration. Therefore, the relaxation terms in (1b) and (2b) may be neglected during the pulse transit through the medium. In this case analytical solutions of the balance equations are known [17]. If the photon flux density at $\xi=0$ (Fig. 1) is $F(0,\eta)$ the pulse shape after the passage through the active medium is given by

$$F(1,\eta)=\frac{A_R F(0,\eta)\,e^{E(0,\eta)}}{1+A_R(e^{E(0,\eta)}-1)}. \tag{3}$$

The photon flux density $F(2,\eta)$ after the pulse passage through the saturable absorber is

$$F(2,\eta)=\frac{B_R F(1,\eta)\,e^{mE(1,\eta)}}{1+B_R(e^{mE(1,\eta)}-1)}. \tag{4}$$

The pulse energy $E(\xi,\eta)=\sigma^a\int_{-\infty}^{\eta}F(\xi,\eta')d\eta'$ is normalized to the active medium saturation energy per unit area of the laser beam $\hbar\omega_L(\sigma^a)^{-1}$. The quantity $m=k\sigma^b/\sigma^a$ contains the ratio k of the beam areas in the amplifying and absorbing media. The inclusion of k allows for telescoping which is employed in some experimental systems to increase the value of m. A_R and B_R are the transmission coefficients at the leading pulse edge in the amplifier and absorber, respectively, during the pulse passage from the right to the left-hand side in the cavity. Analogous expressions are found for the return travel of the pulse. Only A_R and B_R have to be substituted by A_L and B_L. Assuming a small absorber relaxation time T_1^b compared with the cavity transit time U one finds with (1) to (4) the expressions:

$$B_R=B_0, \tag{5}$$

$$B_L=B_0\left\{\frac{[1+A_R(e^{\mathscr{E}_{st}}-1)]^m}{1-B_0+B_0[1+A_R(e^{\mathscr{E}_{st}}-1)]^m}\right\}^{\exp(-U^B/T_1^b)}, \tag{6}$$

$$A_R=A_0\left\{\frac{A_L\{1-B_0B_L+B_0B_L[1+A_R(e^{\mathscr{E}_{st}}-1)]^m\}^{1/m}}{A_0[1-A_L+A_L\{1-B_0B_L+B_0B_L[1+A_R(e^{\mathscr{E}_{st}}-1)]^m\}^{1/m}]}\right\}^{\exp(-U^R/T_1^a)}, \tag{7}$$

$$A_L=A_0\left\{\frac{A_R e^{\mathscr{E}_{st}}}{A_0[1+A_R(e^{\mathscr{E}_{st}}-1)]}\right\}^{\exp(-U^L/T_1^a)}, \tag{8}$$

where $A_0=\exp(\sigma^a\Delta n_0^a L^a)$ and $B_0=\exp(-\sigma^b\Delta n_0^b L^b)$ are the small signal transmissions of the amplifier and absorber, respectively. L is the thickness of the dye jet.

$$\mathscr{E}_{st}=E(0,\eta\to\infty)=\sigma^a\int_{-\infty}^{+\infty}F(0,\eta)d\eta$$

is the pulse energy at $\xi=0$. The propagation times U^R, U^L, U^B are drawn in Fig. 1. Without taking into account the influence of the dispersive element one obtains with (3)–(8) for the photon flux density after one cavity round-trip the relation

$$F(7,\eta)=F(0,\eta)g(E) \tag{9a}$$

with

$$g(E)=\frac{A_R A_L B_0 B_L R\,e^E[1+A_R(e^E-1)]^{m-1}\{1-B_0B_L+B_0B_L[1+A_R(e^E-1)]^m\}^{\frac{1-m}{m}}}{1-A_L+A_L\{1-B_0B_L+B_0B_L[1+A_R(e^E-1)]^m\}^{1/m}}, \tag{9b}$$

where $E=E(0,\eta)$. R is the reflectivity of the output mirror. The transmission of the whole cavity at the leading and trailing edge of the pulse is given by $T_i=g(E=0)=A_R A_L B_0 B_L R$ and $T_f=g(E=\mathscr{E}_{st})$, respectively.
The influence of the bandwidth limiting element on the spectral amplitudes $A(\omega-\omega_L)$ of the pulse during a single passage is described by $A(5,\omega-\omega_L)=H(\omega-\omega_L)A(4,\omega-\omega_L)$. The transfer function $H(\omega-\omega_L)$ is assumed as Lorentzian $H(\omega-\omega_L)=[1+2i(\omega-\omega_L)/\Delta\omega]^{-1}$ with a center frequency ω_L and a bandwidth $\Delta\omega$. Supposing that

the spectral width of the pulse is small enough compared with $\Delta\omega$ the change of the intensity after a double passage through this element is given by

$$F(7,\eta)=R\left\{F(4,\eta)-2\frac{2}{\Delta\omega}\frac{d}{d\eta}F(4,\eta)\right.$$
$$\left.+\left(\frac{2}{\Delta\omega}\right)^2\left[3\frac{d^2}{d\eta^2}F(4,\eta)-\frac{1}{2F(4,\eta)}\left(\frac{d}{d\eta}F(4,\eta)\right)^2\right]\right\}. \tag{10}$$

In the steady-state the pulse shape reproduces itself after one cavity round trip with a possible shift h in the local time. If h is small compared with the pulse duration the steady-state condition may be written in the form

$$F(7,\eta)=F(0,\eta+h)\approx\left[1+h\frac{d}{d\eta}+\frac{h^2}{2}\frac{d^2}{d\eta^2}\right]F(0,\eta). \tag{11}$$

With $F(4,\eta)=R^{-1}F(0,\eta)g(E)$ the combination of (10) and (11) leads to an nonlinear integro-differential equation for the steady state pulse shape $F\equiv F(0,\eta)$:

$$F+h\frac{dF}{d\eta}+\frac{1}{2}h^2\frac{d^2F}{d\eta^2}=Fg-2\frac{2}{\Delta\omega}\frac{d}{d\eta}(Fg)+\left(\frac{2}{\Delta\omega}\right)^2\left[3\frac{d^2}{d\eta^2}(Fg)-\frac{1}{2Fg}\left(\frac{d}{d\eta}Fg\right)^2\right] \tag{12}$$

with $g=g(E)$ corresponding to (9b).
An exact analytic solution of this equation is not possible. We expand the pulse shape near the maximum at $\eta=0$ into a power series. On the other hand, at the edges the gain g is nearly constant ($g=T_i$ and $g=T_f$ at the leading and trailing pulse edge, respectively). Therefore in the wings equation (12) is solved by exponential functions and we make the ansatz:

$$F(0,\eta)=F_0\begin{cases}\frac{1}{2}\exp[\varrho_i(\eta-\eta_i)/\theta] & -\infty<\eta<\eta_i<0\\ 1-(\eta/\theta)^2+\mu(\eta/\theta)^3 & \eta_i\leqq\eta\leqq\eta_f\\ \frac{1}{2}\exp[-\varrho_f(\eta-\eta_f)/\theta] & 0<\eta_f<\eta<\infty\,,\end{cases} \tag{13}$$

where θ and μ are measures for the pulse duration and the asymmetry of the pulse shape, respectively. F_0 is the photon flux density in the pulse maximum. The three time intervalls are fitted at η_i and η_f which are solutions of the equation $1-(\eta/\theta)^2+\mu(\eta/\theta)^3=1/2$. For $|\mu|>\sqrt{8/27}$ a continuous fitting of the parts of the ansatz (13) is not possible. In this case there exists a discontinuity at η_i or η_f. The full width at half maximum τ is given by $\tau=\eta_f-\eta_i$. For nearly symmetrical pulses one obtains $\tau\approx\sqrt{2}\theta$.
Putting this ansatz (13) into (12) and comparing the coefficients of the power η^0 and η^1 we find

$$1-H^2=g_0-2W\sigma^aF_0\theta g_0'-W^2\left[6g_0-3(\sigma^aF_0\theta)^2g_0''+\frac{1}{2g_0}(\sigma^aF_0\theta g_0')^2\right], \tag{14}$$

$$-2H+3\mu H^2=\sigma^aF_0\theta g_0'+W[4g_0-2(\sigma^aF_0\theta)^2g_0'']+W^2[-22\sigma^aF_0\theta g_0'+18\mu g_0+3(\sigma^aF_0\theta)^3g_0'''$$
$$+\frac{1}{2g_0^2}(\sigma^aF_0\theta g_0')^3-\frac{1}{g_0}(\sigma^aF_0\theta)^3g_0'g_0''\Big]. \tag{15}$$

Here we used the following abbreviations: $H=h/\theta$, $W=2/(\Delta\omega\theta)$,

$$g_0=g(E_0),\ g_0'=\left.\frac{dg(E)}{dE}\right|_{E_0},\ g_0''=\left.\frac{d^2g(E)}{dE^2}\right|_{E_0},\ g_0'''=\left.\frac{d^3g(E)}{dE^3}\right|_{E_0},\ E_0=\sigma^a\int_{-\infty}^{0}F(0,\eta)d\eta\,.$$

By integration with respect to η in (12) in two independent ways firstly from $-\infty$ up to $+\infty$ and secondly from $-\infty$ up to 0 one gets

$$\mathscr{E}_{st}=R\ln\{1-A_L+A_L[1-B_0B_L+B_0B_L(1-A_R+A_R\,e^{\mathscr{E}_{st}})^m]^{1/m}\}-\tfrac{1}{4}W^2\sigma^aF_0\theta[T_i\varrho_i+T_f\varrho_f+2.8g_0], \tag{16}$$

$$E_0=R\ln\{1-A_L+A_L[1-B_0B_L+B_0B_L(1-A_R+A_R\,e^{E_0})^m]^{1/m}\}$$
$$-(H+2Wg_0)\sigma^aF_0\theta+W^2[3(\sigma^aF_0\theta)^2g_0'-\tfrac{1}{4}\sigma^aF_0\theta(T_i\varrho_i+1.490)] \tag{17}$$

with

$$\varrho_f = \max\{[H+2T_fW \pm \sqrt{(H+2T_fW)^2-2(1-T_f)(H^2-5T_fW^2)}]/(H^2-5T_fW^2)\},$$

$$\varrho_i = \max\{[-(H+2T_iW) \pm \sqrt{(H+2T_iW)^2-2(1-T_i)(H^2-5T_iW^2)}]/(H^2-5T_iW^2)\}.$$

The last term in (12) provides only a small contribution. To carry out the integration over this term we made the approximation $g=1$ and $\mu=0$ which gives only a small correction. Integration with respect to η in the ansatz (13) from $-\infty$ up to $+\infty$ and from $-\infty$ up to 0 gives the equations

$$\mathscr{E}_{st} = \sigma^a F_0 \theta \left[(\eta_f-\eta_i)/\theta - \frac{1}{3}(\eta_f^3-\eta_i^3)/\theta^3 + \frac{1}{4}\mu(\eta_f^4-\eta_i^4)/\theta^4 + \frac{1}{2\varrho_i} + \frac{1}{2\varrho_f}\right], \tag{18}$$

$$E_0 = \sigma^a F_0 \theta \left[-\eta_i/\theta + \frac{1}{3}(\eta_i/\theta)^3 - \frac{1}{4}\mu(\eta_i/\theta)^4 + \frac{1}{2\varrho_i}\right]. \tag{19}$$

Now we have to solve a system of seven coupled transcendental equations (7) and (14)–(19) for the seven unknown quantities $\mathscr{E}_{st}$ (steady-state pulse energy), E_0 (pulse energy up to the maximum), F_0 (peak intensity), μ (asymmetry parameter), θ (pulse duration), h (time shift), and A_R (amplification at the leading edge of the pulse coming from the right-hand side). The other quantities B_R, B_L, and A_L are explicit functions of A_R and $\mathscr{E}_{st}$ and may be substituted in (7) and (14)–(19) by the expressions (5), (6), and (8).
A similar method as developed here was used for the investigation of the synchronously pumped dye laser in [18].

2. Discussion

We have solved the transcendental equations (7) and (14)–(19) numerically. The results are plotted in Figs. 3–5. The position of the active dye and the absorber within the cavity is fixed by the values of U^R, U^L, and U^B. In our calculations we considered the laser medium in the middle of the cavity ($U^R = U^L$). This is the optimum position for a maximum energy of the pulses (see [19]). The saturable absorber is placed near one end mirror ($U^B=0$) but we considered it as either non-contacted or long compared with the pulse duration. In the case of a short contacted absorber cell coherence effects of the superposition at the incident and reflected part of the pulse should be included in the calculations, this was done in [20] for the case of small absorber loss, small laser gain, and small pulse energy.
In Sect. 2.1 we discuss the conditions for the occurence of mode-locking (stable single-pulse regime), and in Sect. 2.2 we treat the dependence of the pulse properties on the laser parameters.

2.1. Stable Single Pulse Regime

Real solutions of (7) and (14)–(19) corresponding to a stable single pulse regime exist only in a limited range of the parameters A_0, B_0, R, U/T_1^a, and m. (Unphysical branches of solutions, e.g. with $E_0 > \mathscr{E}_{st}$, are excluded.) In Fig. 3a the region of mode-locking is plotted in the $A_0 - B_0$-plane. The boundaries of the region are indicated by solid lines. For small absorber loss $1-B_0 \ll 1$ and small gain $A_0 - 1 \ll 1$ the parameter range for mode-locking is small. Decreasing absorber transmission leads to a broader stability range but on the other side the minimum pump power to reach the mode locking regime increases.
The lower boundary of the mode-locking solutions lies at the chosen values of the laser parameters below the laser threshold $T_0 = A_0^2 B_0^2 R = 1$ which is indicated by a dash-dot line. In order to start the laser oscillation the laser has to be pumped up to threshold, but then the gain can be lowered while the laser oscillates, the laser keeps oscillating in a mode-locked regime even below threshold.
We note that the stable single-pulse region is different from the static pulse compression region defined by a negative net gain on both pulse edges [8, 14]. The boundaries of this region are given by the curves $T_i = g(E=0) = 1$ and $T_f = g(E=\mathscr{E}_{st}) = 1$ indicated by dashed lines and for $B_0 > 0.7$ lie within the stable single-pulse region. This means that the condition of negative net gain on both pulse edges is not a necessary criterion for the occurence of mode-locking. A steady-state pulse solution would also exist in principle with a loss on one of the edges and an amplification on the other. The possibility of such a regime was discussed in [14], but no unique answer on the question of its real existence could be given in the framework of a rate-equation calculation neglecting the influence

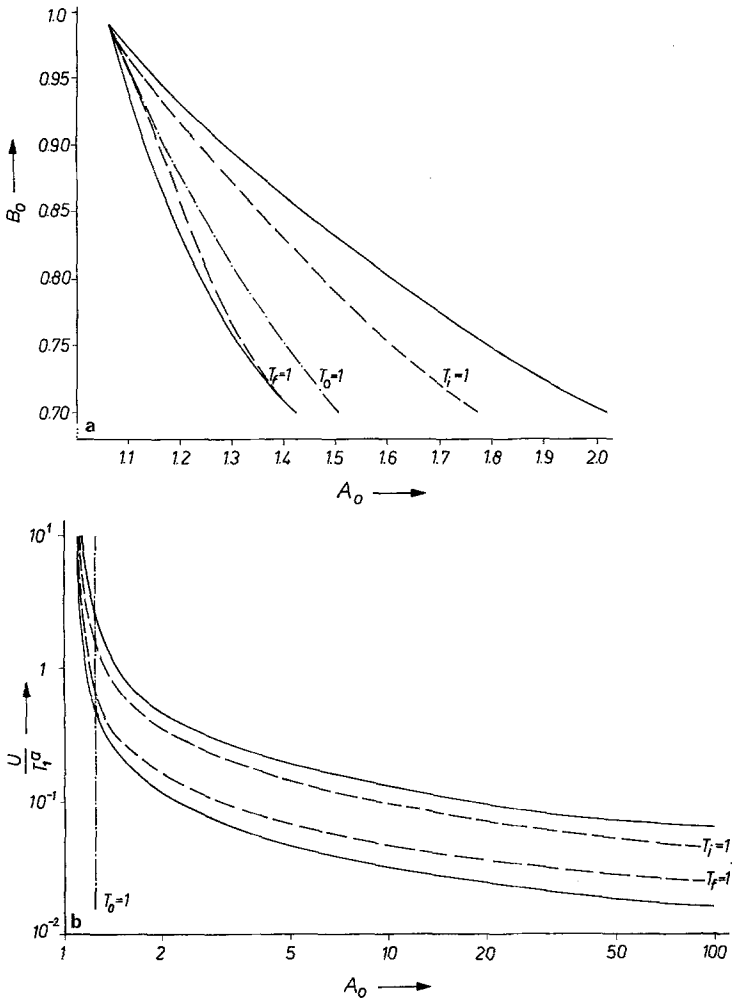

Fig. 3a and b. Stable single-pulse region in the A_0-B_0-plane (a) and in the A_0-U/T_1^a-plane (b). The boundaries of the static pulse compression region ($T_i=1$, $T_f=1$) are indicated by dashed lines. The laser threshold ($T_0=1$) is designated by a dash-dot line. The parameter values are $R=0.9$, $m=7$, $U^B=0$ and $U^L=U^R$. In (a) the cavity length is fixed at $U=T_1^a$, in (b) the absorber transmission is $B_0=0.85$

of bandwidth limitation. In comparison with this the criterion of a real selfconsistent solution of (12) can be considered as a necessary condition for mode-locking. On the other hand, the parameter range of the steady-state mode locked pulse solution is overlaped by the region of self-starting of mode locking from a cw time-independent state of operation in the early stage of the pulse formation process. Such a criterion of self starting characterized by the growth of a periodic perturbation on the time-independent laser output has been derived in [10–12] and can also be considered as a necessary (but not sufficient) condition.

As it can be seen in Fig. 3 the small-signal absorber transmission B_0 has to be smaller than a maximum value $B_0^{\max}$. At the absorber transmission $B_0^{\max}$ the boundaries of the stable single-pulse region and the three curves $T_1=1$, $T_f=1$ and $T_0=1$ end up in one point. This point is characterized by $\mathscr{E}_{st}=0$ and

$$\left.\frac{dT_i}{d\mathscr{E}_{st}}\right|_{\mathscr{E}_{st}=0} = \left.\frac{dT_f}{d\mathscr{E}_{st}}\right|_{\mathscr{E}_{st}=0}.$$

Using these conditions we find after some calculation

$$B_0^{\max} = \sqrt{1+\frac{1}{4R}\left(\frac{1-R}{m-1}\right)^2} - \frac{1-R}{2\sqrt{R}(m-1)}. \tag{20}$$

For the parameters $R=0.9$ and $m=7$ one gets $B_0^{\max}=0.991$. In Fig. 3b the stable single-pulse region is shown in the $U/T_1^a-A_0$-plane. The width of the stable single-pulse region depends very sensitively on the value of the cavity length U/T_1^a. For very long cavities $U/T_1^a \gg 1$ the region of the cw stable single pulse regime tends below threshold and becomes very narrow. Very short cavities are also unfavourable because the minimum pumping power for reaching the stability region becomes very large.

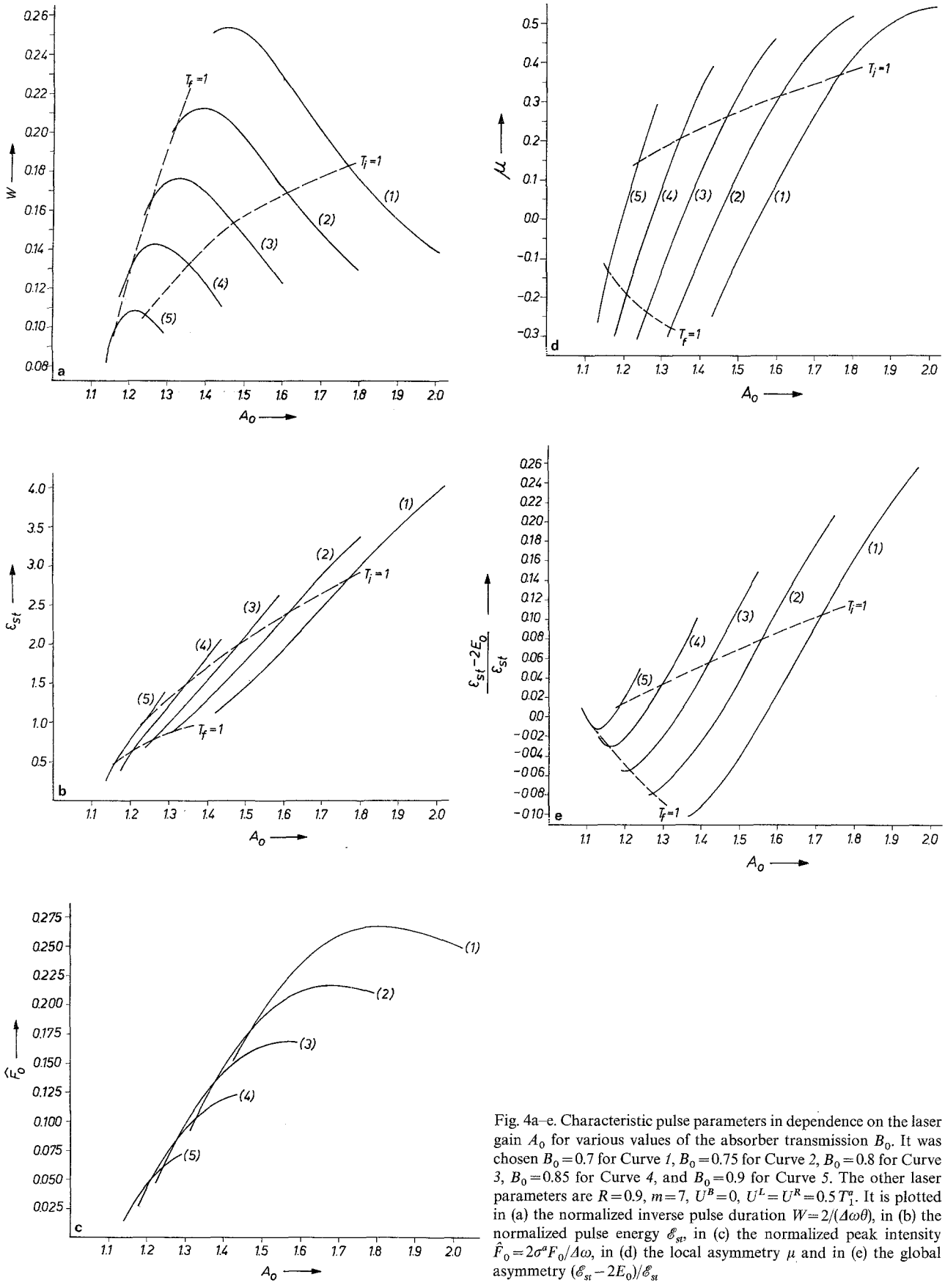

Fig. 4a–e. Characteristic pulse parameters in dependence on the laser gain A_0 for various values of the absorber transmission B_0. It was chosen $B_0=0.7$ for Curve *1*, $B_0=0.75$ for Curve *2*, $B_0=0.8$ for Curve *3*, $B_0=0.85$ for Curve *4*, and $B_0=0.9$ for Curve *5*. The other laser parameters are $R=0.9$, $m=7$, $U^B=0$, $U^L=U^R=0.5\,T_1^a$. It is plotted in (a) the normalized inverse pulse duration $W=2/(\Delta\omega\theta)$, in (b) the normalized pulse energy $\mathcal{E}_{st}$, in (c) the normalized peak intensity $\hat{F}_0=2\sigma^a F_0/\Delta\omega$, in (d) the local asymmetry μ and in (e) the global asymmetry $(\mathcal{E}_{st}-2E_0)/\mathcal{E}_{st}$

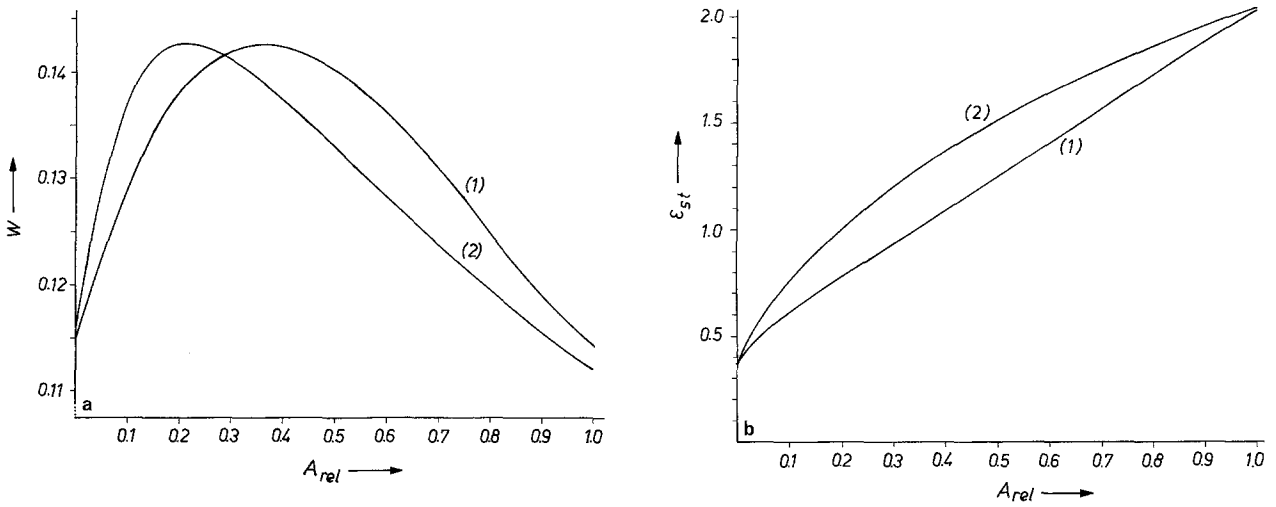

Fig. 5a and b. Inverse pulse duration $W=2/(\Delta\omega\theta)$ (a) and pulse energy $\mathcal{E}_{st}$ (b) in dependence on the laser gain for $U/T_1^a=1$ (Curve *1*) and $U/T_1^a=0.1$ (Curve 2). The normalized gain factor A_{rel} is explained in the text. The laser parameters are $B_0=0.85$, $R=0.9$, $m=7$, $U^B=0$, and $U^R=U^L$

2.2. *Pulse Parameters*

We shall now discuss the dependence of the pulse properties on the laser, absorber and resonator parameters. In Fig. 4a the inverse pulse duration in dimensionless unites is plotted $[W=2/(\Delta\omega\theta)]$ as a function of the small signal gain A_0 for various values of the small-signal loss B_0 and fixed values of $m=7$, $R=0.9$. The end points of the curves characterize the end of the stable single-pulse region. As discussed in the last section, the boundaries of the static pulse compression region $T_i=1$ and $T_f=1$, indicated by dashed lines, lie inside the stable single-pulse regime. For small values of A_0 the pulse duration decreases with increasing pump power (increasing A_0). After reaching a minimum value a further increase of pumping power leads to an increase of the pulse durations. Decreasing absorber transmission B_0 results in the generation of shorter and more intensive pulses. The minimum of the pulse duration tends for smaller B_0 to the left boundary of the mode locking region. This behaviour is in agreement with experimental results in [4], where at higher pumping power levels an increase of the pulse duration has been observed.

The variation of the pulse duration in dependence on the intracavity bandwith $\Delta\omega$ is given by the relation $\theta\sim(\Delta\omega)^{-1}$. The pulse energy $\mathcal{E}_{st}$ increases monotonously with the small-signal gain A_0 (Fig. 4b). For small absorber loss the intensity also increases monotonously with growing pumping power but at higher absorber loss the intensity reaches a maximum within the stable single-pulse region (Fig. 4c).

The quantities μ (Fig. 4d) and $(\mathcal{E}_{st}-2E_0)/\mathcal{E}_{st}$ (Fig. 4e) are measures of the asymmetry at the pulse shape: μ is a local measure near the pulse peak whereas $(\mathcal{E}_{st}-2E_0)/\mathcal{E}_{st}$ is a global measure. Comparing with the pulse duration in Fig. 4a one can see that for $B_0\gtrsim 0.8$ the pulse is nearly symmetrical ($\mu\approx 0$ and $\mathcal{E}_{st}-2E_0\approx 0$) if the pulse duration takes its minimum value. Reducing the pumping power below this point of minimum pulse duration leads to a steepening of the trailing edge ($\mu<0$, $E_0>\mathcal{E}_{st}/2$), whereas a higher small-signal gain results in a steepening of the leading edge ($\mu>0$, $E_0<\mathcal{E}_{st}/2$). This behaviour could be expected since a higher gain leads to a higher amplification of the leading pulse edge.

As an example we calculate the pulse parameters for a filter bandwidth $\Delta\omega=5\times 10^{13}$ Hz, a cross section for stimulated emission $\sigma^a=3\times 10^{-16}\,\mathrm{cm}^2$, a beam diameter of 15 µm within the active dye and a wavelength $\lambda=600$ nm of the laser radiation, which are characteristic values for mode-locked Rhodamine-6G-dye lasers. The other laser parameters are chosen to be $A_0=1.3$, $B_0=0.85$, $R=0.9$, $m=7$, $U^B=0$, and $U^R=U^L=0.5\,T_1^a$. We find for the pulse duration $\theta=0.28$ ps. The pulse energy and peak power outside the cavity are 2.4×10^{-10} J and 470 W, respectively. The asymmetry of the pulse can be taken from Fig. 4d and e. The local asymmetry is $\mu=0.075$, the global asymmetry $(\mathcal{E}_{st}-2E_0)/\mathcal{E}_{st}=0.002$.

Figure 5a and b show the dependence of the pulse duration and the pulse energy on the laser gain for two values of the ratio U/T_1^a. Since the width of the mode-locking region strongly depends on this ratio we have normalized the gain $A_{rel}=(A_0-A_{min})/(A_{max}-A_{min})$, where A_{min} and A_{max} are the values of the small-signal gain A_0 at the lower and upper limit of the stable single-pulse region. Figure 5 shows that the pulse parameters do not sensitively depend on the ratio of cavity round-trip time U over recovery time T_1^a of the active dye.

Finally we will give a short comparison of our results with those of Haus [13]. Haus used the approximations of small gain, small absorber loss and small pulse energy:

$$1-B_0 \ll 1, \quad A_0-1 \ll 1, \tag{21a}$$

$$\mathscr{E}_{st} \ll 1, \quad m\mathscr{E}_{st} \ll 1. \tag{21b}$$

In this approximation the pulse duration decreases monotonously with increasing laser gain. Comparing with Fig. 4a one finds that at the chosen laser parameter such a behaviour can be observed only near the lower limit of the stable single-pulse regime. Considering the pulse energy in Fig. 4b we see that at $m=7$ even for small amplification and low absorber loss the condition (21b) is not fulfilled. There is a strong limitation of the validity of the solution given in [13]. Only for small values of m there can be found a small region in which the conditions (21) are fulfilled. But in order to have optimum conditions the region of larger values of m, A_0, and $\mathscr{E}_{st}$ is of greater experimental interest.

In order to give a test for the ansatz (13) we simplify (5)–(8) and (14)–(19) using the conditions (21) and compare with the equations in [13, 20]. After some calculation we can eliminate two of the variables by the solution $E_0=\sigma^a F_0\theta=\mathscr{E}_{st}/2$. This leads to $\mu=0$. These relations would also be obtained using a secant-hyperbolic pulse shape. For the other equations we find

$$\begin{aligned} 1+2H+2H^2 &= f_0(1-4W)+W^2(12f_0-S), \\ -2H &= \tfrac{1}{2}f'_0\mathscr{E}_{st}+\tfrac{1}{4}f''_0\mathscr{E}_{st}^2+4Wf_0+2Wf'_0\mathscr{E}_{st}, \\ 3H^2 &= \tfrac{1}{8}f''_0\mathscr{E}_{st}^2+3Wf'_0\mathscr{E}_{st}+W^2(18f_0-S) \end{aligned} \tag{22}$$

with

$$H=h/\theta,\ W=2/(\Delta\omega\theta),\ f_0=1+\alpha_R+\alpha_L-\varkappa_0-\varkappa_L-\gamma,\ f'_0=m(\varkappa_0+\varkappa_L)-\alpha_R-\alpha_L,\ f''_0=-m^2(\varkappa_0+\varkappa_L),$$

$$\alpha_{R/L}=\alpha_0\left[1-\frac{\exp(U^{L/R}/T_1^a)+1}{\exp(U/T_1^a)-1}\mathscr{E}_{st}\right],\ \alpha_0=\ln A_0,$$

$$\varkappa_L=\varkappa_0\{1-[m\mathscr{E}_{st}-\tfrac{1}{2}(m\mathscr{E}_{st})^2]\exp(-U^B/T_1^b)\},\ \varkappa_0=-\ln B_0,$$

$$\gamma=-\ln R \quad \text{and} \quad S=3(T_i\varrho_i+T_f\varrho_f+2.8g_0)/8.$$

The special form of S results from the approximate integration over the last term in (12). Comparing with [13] it should be noted that in this paper a gaussian transfer function for the dispersive element has been used (without first-order derivations in the local time) and only linear terms in H have been considered. Therefore, (22) should be better compared with the results in [20], where the same suppositions as here has been used. There would be an exact correspondence if we set $S=2f_0$. This is only a small deviation in a second-order term from the equations derived with the approximations (21) and a secanthyperbolic pulse shape ansatz. Therefore, within the range of validity of the solution given by Haus we obtain a good correspondence with our ansatz (13).

References

1. W.Schmidt, F.P.Schafer: Phys. Lett. **26**A, 558 (1968)
2. D.J.Bradley, F.O'Neill: Opto-electronics **1**, 69 (1969)
3. C.V.Shank, E.P.Ippen: Appl. Phys. Lett. **24**, 373 (1974)
4. I.S.Ruddock, D.J.Bradley: Appl. Phys. Lett. **29**, 296 (1976)
5. J.C.Diels, E. van Stryland, G.Benedict: Opt. Commun. **25**, 93 (1978)
6. I.S.Ruddock: Appl. Opt. **18**, 3212 (1979)
7. E.G.Arthurs, D.J.Bradley, P.N.Puntambekar, I.S.Ruddock, T.J.Glynn: Opt. Commun. **12**, 360 (1974)
8. G.H.C.New: Opt. Commun. **6**, 188 (1972)
9. G.H.C.New: IEEE J. Quant. Electron. **10**, 115 (1974)
10. B.K.Garside, T.K.Lim: J. Appl. Phys. **44**, 2335 (1973)
11. G.H.C.New, D.H.Rea: J. Appl. Phys. **47**, 3107 (1976)
12. H.A.Haus: IEEE J. Quant. Electron. **12**, 169 (1976)
13. H.A.Haus: IEEE J. Quant. Electron. **11**, 736 (1975)
14. G.H.C.New, K.E.Orkney, M.J.W.Nock: Opt. Quant. Electron. **8**, 425 (1976)
15. R.Muller, E.Neef: Ann. Phys. Leipzig **34**, 37 (1977)
16. R.Muller: Opt. Commun. **28**, 259 (1979)
17. L.M.Frantz, J.S.Nodvick: J. Appl. Phys. **34**, 2346 (1963)
18. J. Herrmann, U.Motschmann: Appl. Phys. **27**, 27 (1981)
19. F.Weidner, J.Herrmann: Exp. Technik der Physik (to be published)
20. J.Herrmann, F.Weidner, B.Wilhelmi: Appl. Phys. B**26**, 197 (1981)

Responsible for Advertisements: E. Lückermann, G. Probst, Kurfürstendamm 237, D-1000 Berlin 15, Telephone: (030) 8821031, Telex 01-85411
Springer-Verlag Berlin–Heidelberg–New York. Printers: Brühlsche Universitätsdruckerei, Giessen, Printed in Germany

Beihefterhinweis: Dieser Ausgabe ist ein Prospekt des Springer-Verlages beigeheftet.